



Adam CAUSSE

Promotion P2026 - 4^{ème} année



Rapport de Stage Elève-Ingénieur

Develop methods for micro/nanofabrication of topographic gradient surfaces using a femto-second laser.

University of Otago – Dunedin – New-Zealand

12/08/2024 – 20/12/2024

Energy Research Physics Department

Tutor: Sam Lowrey

Acknowledgement

I would like to begin by expressing my gratitude to my tutor, Sam Lowrey, for giving me the opportunity to do this internship in his laboratory.

I would also like to thank Kirill Misiuk for the trust he placed in me in using expensive equipment, as well as for sharing his valuable advice.

I would also like to thank all my colleagues in the research team, who helped maintain a working atmosphere that was both friendly and conducive to the emergence of good ideas.

Finally, I would like to warmly thank the entire team of the physics department for their warm welcome and their support in all the tasks accomplished.

Table of Content :

Acknowledgement.....	1
Table of Content :	2
Table of Figures :	3
Table of tables :	4
Table of Equations :	4
I. Introduction :	6
II. Presentation of the Company :	7
III. Research Project :	8
Context :	8
Concept of Contact Angle:	8
Theory :	9
Status of progress:	11
Equipements :	12
Laser Femtoseconde :	12
Scanning Electron Microscope:.....	14
Goniometer :	15
Ultrasonic Bath :	16
Sample Storage :	16
Study of engravings with the short-range lens:	17
Study of Single Channels :	17
Creation of superhydrophobic surfaces:.....	19
Measurements and Limits :	21
Study of engravings with a long-range lens :	24
Study of engravings on single channels :	24
Creation of superhydrophobic surfaces:.....	28
Measurements and Limits :	29
Gradient Creation :	31
Theory :	31
Study and Measurements :.....	32
Comparison of gradients:	41
Study of Glass Engravings :	41
Study of unique channels :	41
Creation of an engraved surface :.....	43
Measurements and Limits :	44
Conclusion :	45

Technical Conclusion :	45
Personal Conclusion :	46
Bibliography	46
Appendix :	47
Appendix 1 :	47
Appendix 2 :	48

Table of Figures :

Figure 1 Drop on a surface	8
Figure 2 Different types of Contact Angle	9
Figure 3 Wenzel's state on the left and Cassie-Baxter's state on the right.....	10
Figure 4 Femtosecond Laser Femtolux 30	12
Figure 5 Laser setup in the room.....	12
Figure 6 DMC Software Interface	13
Figure 7 Long range lens setup	13
Figure 8 Short Range lens setup.....	13
Figure 9 Scanning Electron Microscope setup.....	14
Figure 10 Goniometer OCA-15 Setup.....	15
Figure 11 DMC Software Interface	16
Figure 12 different shapes of channels made with a single repetition.....	17
Figure 13 Cross Section two repeats sample.....	19
Figure 14 Cross Section three repeats Samples.....	20
Figure 15 Goniometry test on two repeats sample	21
Figure 16 Goniometry test on three repeats samples.....	22
Figure 17 Laser Marking Parameters Window.....	25
Figure 18 SEM Image of the Single channel of the red cell.....	26
Figure 19 SEM image of the impact of the deceleration of the laser	27
Figure 20 Cross Section of a sample engraved in 25min	28
Figure 21 Goniometry test on 25min engraving Sample.....	29
Figure 22 Graph Dynamic Contact angle in parallel position	30
Figure 23 Graph Dynamic Contact Angle perpendicular position	30
Figure 24 surface gradient example	31
Figure 25 Screenshot Tracking video SDG1	32
Figure 26 Graphs of the video for gradient SDG1	33
Figure 27 Screenshot of the tracking video of SDG1_Mod gradient	34
Figure 28 SEM images of SDG1_Mod gradient	35
Figure 29 Graphs of the gradient SDG1_Mod	36
Figure 30 Screenshot tracking video of LDG4 gradient.....	37
Figure 31 Graphs of the gradient LDG4.....	38
Figure 32 Screenshot Tracking video of LDG4_Mod	39
Figure 33 SEM Images of LDG4_Mod.....	39
Figure 34 Graphs of the gradient LDG4_Mod	40
Figure 35 Channel of the red Cell	42
Figure 36 Cross section of an engraved glass sample	43
Figure 37 Goniometry test on non-processed glass.....	44
Figure 38 Goniometry test on processed glass	44

Table of tables :

Tableau 1 Distribution of postgraduates Student in 2016.....	7
Tableau 2 single repeat channel data spreadsheet	17
Tableau 3 multiple repeats channel data spreadsheet	18
Tableau 4 Spreadsheet Contact Angle on three repeats samples	22
Tableau 5 Spreadsheet Dynamic Contact Angle.....	23
Tableau 6 Spreadsheet datas Long-Range Lens	24
Tableau 7 Spreadsheet Speed Test Long-Range Lens	26
Tableau 8 Spreadsheet goniometry test of the 25min engraving sample.....	29
Tableau 9 Spreadsheet Single channels engraving on glass samples	41
Tableau 10 Spreadsheet of the speed test on glass sample.....	42

Table of Equations :

Équation 1 Young Equation.....	9
Équation 2 Wenzel Roughness Equation.....	10
Équation 3 Wenzel Equation	10
Équation 4 Result of Wenzel Equation.....	10
Équation 5 Cassie-Baxter Equation.....	11
Équation 6 Cassie-Baxter Equation simplified.....	11
Équation 7 Cassie-Baxter Equation used for the internship.....	11

Intitulé du stage :

Develop methods for micro/nanofabrication of topographic gradient surfaces using a femto-second laser.

Résumé :

Ce stage porte sur la création de gradients surfaciques sur des échantillons d'aluminium. Le projet a débuté par l'étude de l'impact des paramètres laser sur la forme de la surface des échantillons. Dans un second temps, une analyse de l'hydrophobie de surfaces plus larges a permis de développer et d'étudier quatre types de gradients différents.

En parallèle, un projet annexe a été mené pour examiner la réaction du verre à un traitement similaire.

Mots clés : gradient, laser femtoseconde, angle de contact, hydrophobie

Abstract :

This internship focuses on the creation of surface gradients on aluminum samples. The project began with the study of the impact of laser parameters on the surface shape of the samples. In a second step, an analysis of the hydrophobicity of larger surfaces allowed the development and study of four different types of gradients.

In parallel, a side project was conducted to examine the reaction of glass to a similar treatment.

Keywords: gradient, femtosecond laser, contact angle, hydrophobicity

I. Introduction :

Controlling surface hydrophobicity is a major challenge for the development of more sustainable and energy-efficient systems. By limiting interactions between solid surfaces and liquids, hydrophobic properties reduce wear, corrosion, and deposit accumulation, while improving heat exchange performance. Consequently, they find essential applications in various fields, such as energy, microelectronics, aeronautics, and health.

Since the early 2000s, the emergence of femtosecond laser technology has offered a new perspective for the creation of hydrophobic surfaces. These lasers allow surface structuring at the micro- and nanometric scale, paving the way for more precise, repeatable, and more environmentally friendly industrial processes compared to traditional methods. Controlling the morphology of the engraved patterns directly influences the wettability properties, making it possible to achieve high levels of hydrophobicity, or even superhydrophobicity, without resorting to additional chemical treatments.

This technological and scientific context provides the framework for this internship, carried out under the supervision of Dr. Sam Lowrey within his research team in Dunedin, New Zealand. A specialist in the optimization of heat exchangers, Dr. Lowrey focuses his work on the design of more efficient systems by exploiting heat transfer phenomena and liquid-solid interactions. His team also explores mechanisms for improving the durability of functional surfaces, which is part of a desire to solve industrial problems related to energy efficiency and reducing the environmental footprint. During this internship, the main project focuses on the creation of surface gradients on aluminum samples using a femtosecond laser. This work includes the study of the impact of laser parameters on the shape of the etched channels, followed by an in-depth analysis of the hydrophobic properties of these surfaces. The objective is to develop and evaluate four different types of gradients to identify the most promising configurations in terms of durability and functional efficiency. At the same time, a study is being conducted on the reaction of glass to a similar laser treatment, allowing the scope of application of these technologies to be broadened.

This report presents the framework of this research, the methodologies used, and the results obtained. It is part of an approach aimed at contributing to the industrialization of functional surfaces while meeting current challenges of sustainability and energy efficiency.

II. Presentation of the Company :

The University of Otago's Department of Physics, the first of its kind in New Zealand, was established in July 1871, when physics was already a core subject. Today, it is distinguished by innovative teaching methods, rigorous research and a strong commitment to physics as a science and its many applications. Its overarching ambition is to provide students with an exceptionally high-quality education while producing internationally recognised research.

Located in Dunedin, a vibrant university city where the University of Otago's 20,000 students play a key role in the local community, the Department is housed in the modern, purpose-built Science III building, shared with the Department of Mathematics and Statistics, within the Division of Science.

The department's research activities span a wide range of areas, from the theoretical study of ultracold atoms to the fabrication of electronic microtags for tracking animal species such as seabirds.

This framework of excellence attracts talented international postdoctoral researchers who work closely with senior faculty, while an active community of postgraduate students organizes enriching academic and social events.

Postgraduate Student Profile in 2016			
Level	Number of Students	Female	International
PhD	35	31%	51%
MSc	11	3%	1%
400-level	18	17%	17%

Tableau 1 Distribution of postgraduates Student in 2016

The large share of international Postgraduate Students allows for working in a diverse and culturally rich environment.

Sam Lowrey holds a degree in physics from the University of Otago, where he also obtained his PhD in 2012. Following his studies, he held a research position at Otago, developing an optical lithography system for large-area imaging in the evanescent wave regime. Between 2016 and 2021, he led several industry and government-funded projects in the areas of applied thermodynamics and free-surface microfluidics. In October 2021, he joined the University's Department of Physics as a Senior Lecturer.Reaserch interest :

Microfluidics – development of novel micro-/nano-fabricated surfaces for controlling frost and ice formation via surface tension gradients. Passive control of droplets and bubbles on open surfaces.

Engineering Thermodynamics – computational fluid dynamics modelling and performance testing of novel heat exchanger technology. Design, development and performance testing of energy efficient heat pump technology configured for drying processes.

Optical Lithography – development of advanced interference based optical lithographic imaging techniques for nanofabrication. Specific areas include high and ultra-high NA lithography using liquid-immersion and solid-immersion techniques.

III. Research Project :

Context :

Concept of Contact Angle:

The contact angle is an angle measurement used to quantify the wettability of a surface. The closer it is to 180° , the more hydrophobic the surface is. Conversely, the closer the contact angle is to 0, the more hydrophilic the surface is.

The contact angle is defined by the angle formed between the surface of the solid and the surface of the liquid.

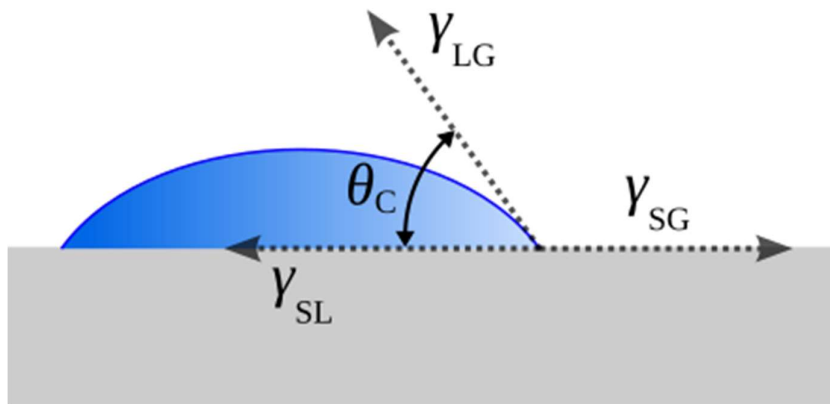


Figure 1 Drop on a surface

This angle allows surfaces to be classified by their hydrophobicity:

- Superhydrophilic surfaces: contact angle < 10°
- Hydrophilic surfaces: contact angle < 90°
- Hydrophobic surfaces: contact angle > 90°
- Superhydrophobic surfaces: contact angle > 150°

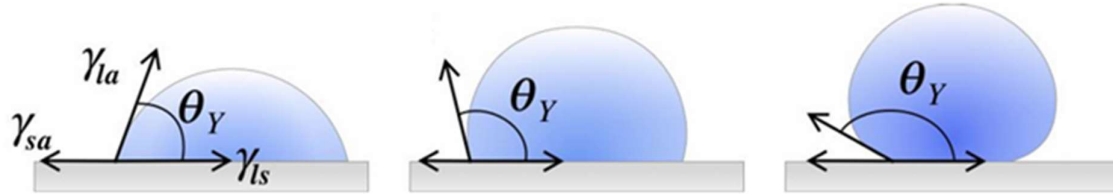


Figure 2 Different types of Contact Angle

The contact angle of a flat aluminum surface is approximately 60°.

Theory :

According (Misiuk, 2023) to Young-Dupré's laws, the value of the contact angle between a flat surface and a drop is defined by the following formula:

$$\cos\theta = \frac{\gamma_{SA} - \gamma_{LS}}{\gamma_{LA}}$$

Équation 1 Young Equation

Where γ_{SA} ; γ_{LS} ; γ_{LA} are the surface tensions between solid and air, liquid and solid, liquid and air. The angle formed by γ_{LS} and γ_{LA} is called the contact angle (θ).

Wenzel's law allows to take into account the roughness of the surface.

It defines roughness (r) as the ratio between real surface (A_{SL}) and projected surface (A_f).

$$r = \frac{A_{SL}}{A_f}$$

Équation 2 Wenzel Roughness Equation

He then obtains the formula :

$$dG = r(\gamma_{SA} - \gamma_{LS}) dx - \gamma_{LA} \cos \theta_W dx$$

Équation 3 Wenzel Equation

With $dG/dx=0$ and Young Equation, we find:

$$\cos \theta_W = r \cos \theta_Y$$

Équation 4 Result of Wenzel Equation

It is then possible to increase the hydrophobicity of a surface by modifying its roughness.

Wenzel's law does not allow to model all surfaces. Indeed, it is necessary to use the Cassie-Baxter law when air pockets form between the surface and the drop.

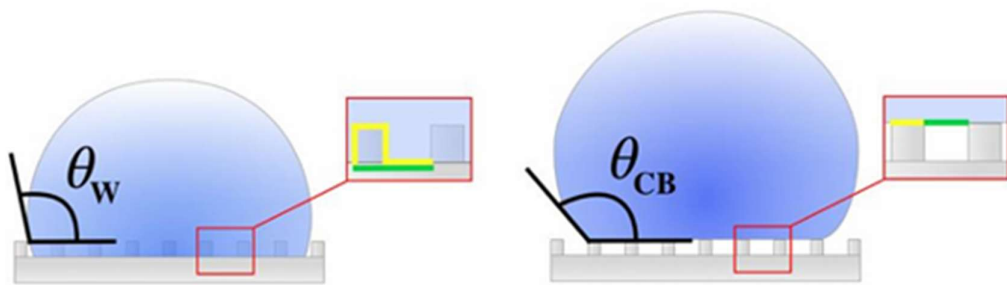


Figure 3 Wenzel's state on the left and Cassie-Baxter's state on the right

Cassie-Baxter's state follows the following formula :

$$dG = f_1(\gamma_{SA} - \gamma_{SL})_1 dx + f_2(\gamma_{SA} - \gamma_{SL})_2 dx - \gamma_{LA} \cos \theta_{CB} dx$$

Équation 5 Cassie-Baxter Equation

Where f_1 and f_2 are the areas of the fractional surfaces (respectively green line and yellow line in figure 4).

With $dG/dx=0$ and Young Equation, we find:

$$\cos \theta_{CB} = f_1 \cos \theta_1 + f_2 \cos \theta_2$$

Équation 6 Cassie-Baxter Equation simplified

Where θ_1 and θ_2 are contact angles of f_1 and f_2 area fractions respectively.

Here, the 2 surfaces are the surface and air pockets. However, the contact angle of a drop in the air is 180° ($\cos \theta_2 = -1$). f_1 is replaced by the area of the fractionnal surface of the element f or $f_1 + f_2 = 1$ so $f_2 = 1 - f_1$

All this allows us to obtain:

$$\cos \theta_{CB} = -1 + f(1 + \cos \theta_Y)$$

Équation 7 Cassie-Baxter Equation used for the internship

The objective of this internship is to increase the hydrophobicity of surfaces by increasing their roughness(case of Wenzel's state) or creating air pockets under the droplet to limit the interaction between the droplet and the surface(Cassie-Baxter's state). To do this, it was decided to create parallel channels over the entire surface.

Status of progress:

The previous internship started the study of the shape of these channels by varying the laser parameters. This study allowed to discover the femtosecond laser and to carry out the first Goniometry tests to measure the first contact angles. The best samples allowed to obtain angles of 120° .

Equipements :*Laser Femtoseconde :*

The femtosecond laser is a technology that has been developing since the early 2000s. The model used for this internship is the Femtolux 30. Adapted to industrial needs.



Figure 4 Femtosecond Laser Femtolux 30

This laser must be combined with a network of mirrors and lenses as well as a 3-axis platform to be usable.

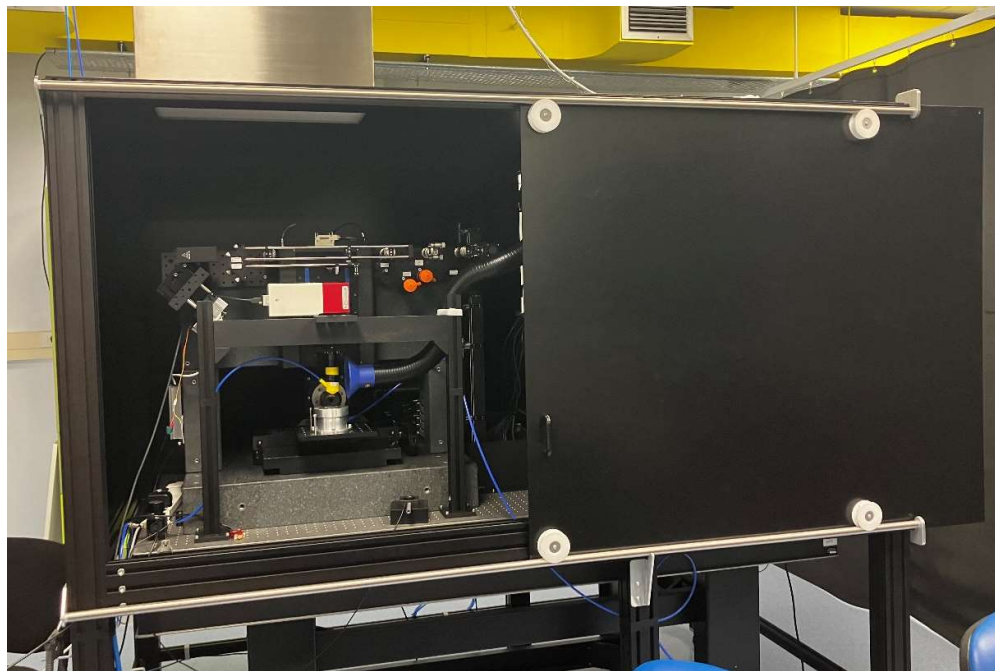


Figure 5 Laser setup in the room

This laser produces pulses of about 300fs with a released energy of up to $60\mu\text{J}$ per pulse. This allows for very precise engraving. The software used to manipulate the laser is DMC. This is easy to use when you have already done CAD.

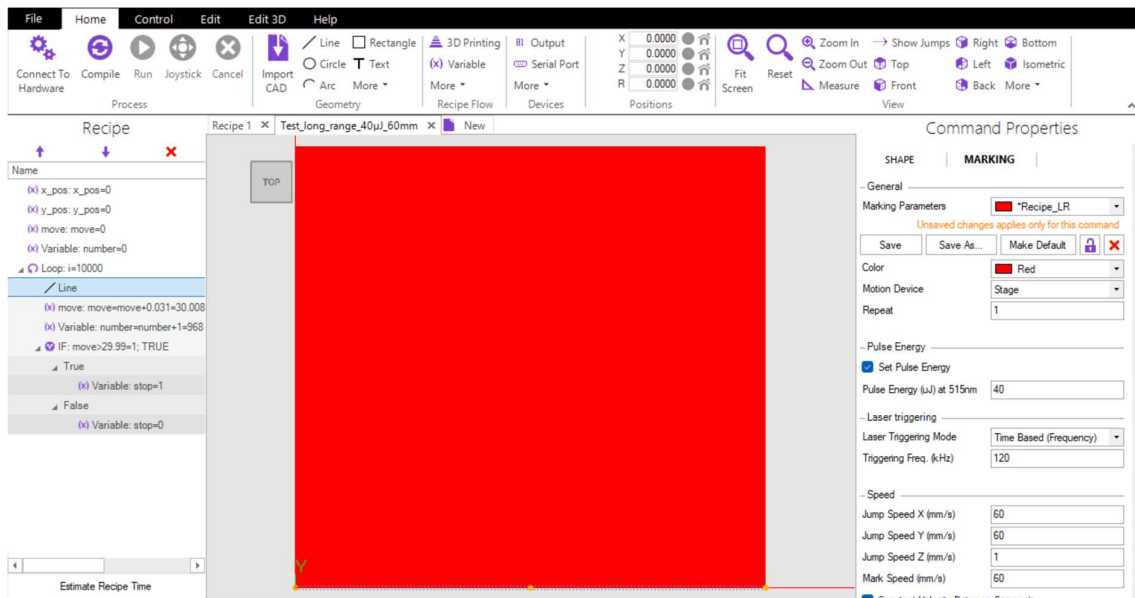


Figure 6 DMC Software Interface

The interface is divided into three parts: the left for the movements that the laser will perform, the right for the frequency, speed and energy parameters of the laser. The middle is dedicated to a WYSIWYG visualization of the model. It is possible to change the size of the laser lens. During this internship, a lens with a focal length of 50mm (we will call it a short-range lens) and a lens with a focal length of 100mm (we will call it a long-range lens) were used.

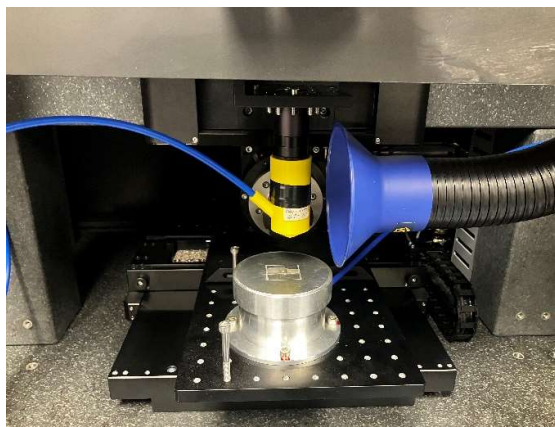


Figure 7 Long range lens setup

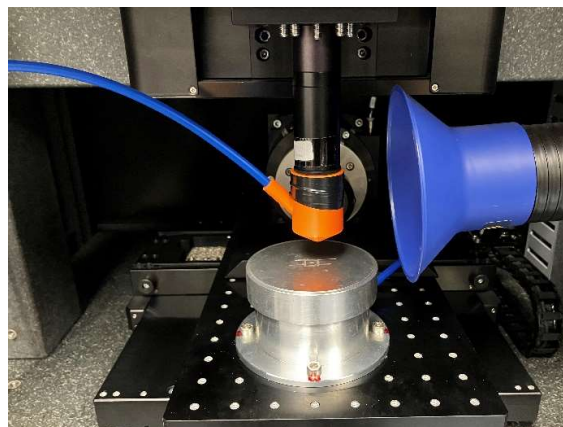


Figure 8 Short Range lens setup

Scanning Electron Microscope:

In the search for the ideal channel shape for surface hydrophobicity, it is necessary to be able to measure each test precisely. For this, the scanning electron microscope is essential.

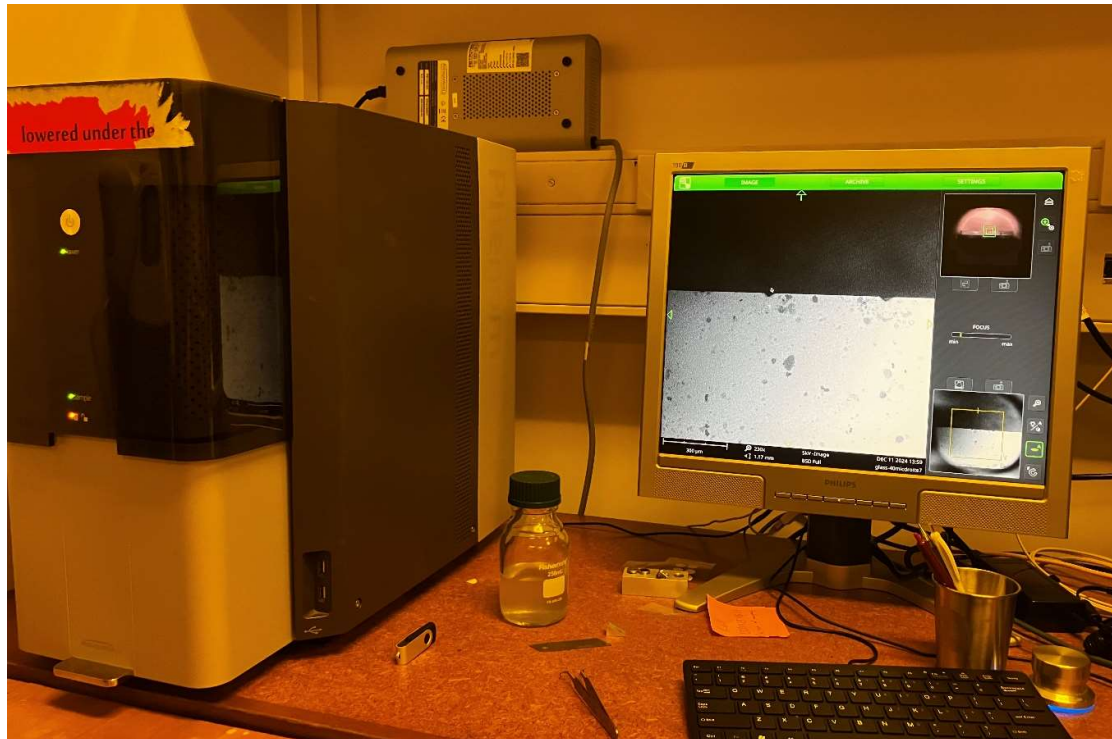


Figure 9 Scanning Electron Microscope setup

The software allows you to take measurements directly on freshly taken images.

Goniometer :

The goniometer is a very complete tool for characterizing the wettability of a surface.

The goniometer is an OCA-15 developed by DataPhysics

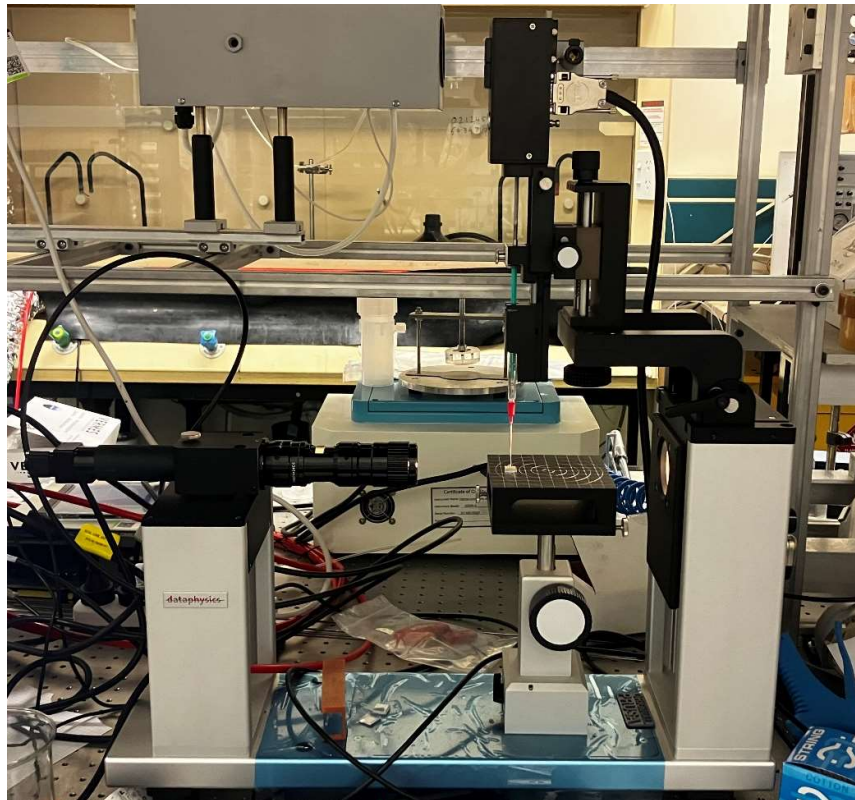


Figure 10 Goniometer OCA-15 Setup

It is composed of a syringe whose volume of water ejected can be chosen.

An adjustable platform and a camera allowing to make videos with different precisions.

A software (DPI Max) accompanies the use of this tool where we can measure the contact angles in different ways.

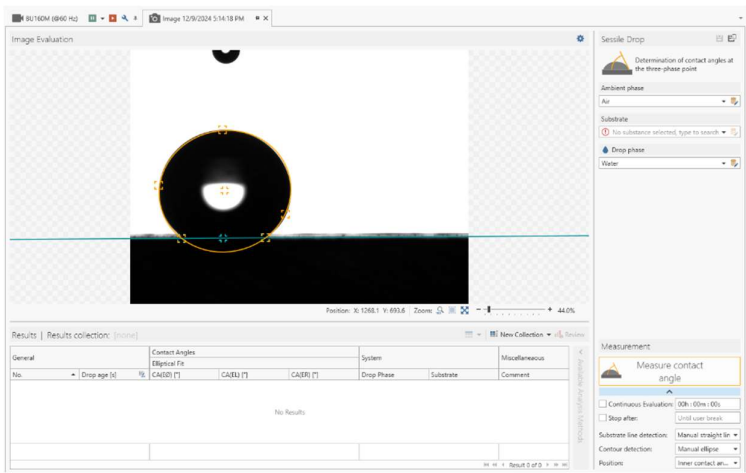


Figure 11 DMC Software Interface

The right side of the interface is dedicated to settings (liquid type, drop volume, measurement technique).

Ultrasonic Bath :

The ultrasonic bath is used to clean the samples after etching. After etching, the sample was placed in a vial of Isopropanol and then the whole thing was placed in the ultrasonic bath filled with water.

For aluminum samples, the washing time was between 10 and 15 minutes and for glass samples, the washing time was 20 minutes.

Sample Storage :

The aluminum samples are stored in an airtight box to isolate them from the ambient air. A few drops of fruit acid (Jiangyou Long, 2014) are placed in the center of the box to enrich the atmosphere of the box. This technique increases the oxidation speed of the etched surface.

Study of engravings with the short-range lens:

Study of Single Channels :

The study of single channels is essential to be able to find the right parameters of the femtosecond laser. In this study, a study of single channels was first carried out with a single repetition:

		Beam energy									
frequency	1μJ	2μJ	5μJ	10μJ	20μJ	30μJ	40μJ	50μJ	60μJ	70μJ	
5kHz	width:10.2 depth:0		width:17.9 depth:0	width:17.6 depth:5.62	width:22.6 depth:5.01			width:28.2 depth:7.31		width:37.5 depth:8.15	
10kHz					width:13.5 depth:9.35						
20kHz			width:17 depth:7	width:16 depth:3.41	width:20.7 depth:18.2			width:27.6 depth:22.5			
40kHz	width:13.3 depth:4.11		width:16.6 depth:12.4		width:19 depth: ?			width:35.7 depth: ?	width:30.7 depth: ?		
60kHz					width:17.1 depth:4.77						
80kHz					width:16.9 depth:4.86						
100kHz	width:12.8 depth:7.72	width:11.4 depth:2.27	width:15.7 depth: ?	width:16 depth:3.41	width:16.3 depth: ?	width:21.1 depth:6.43	width:25.2 depth:3.69	width:19 depth: ?	width:29 depth:4.88	width:17.5 depth: ?	
120kHz					width:16.8 depth:4.5						
140kHz					width:19.2 depth:3.46						
					width:19.3						

Tableau 2 single repeat channel data spreadsheet

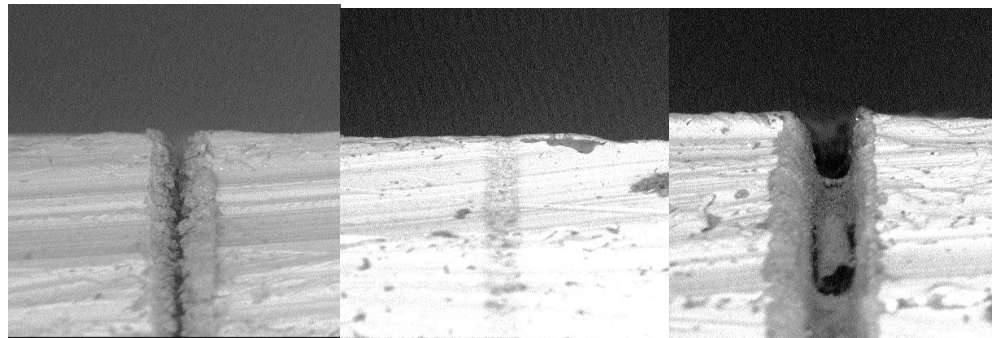


Figure 12 different shapes of channels made with a single repetition

This first study was long because it required finding the right focus to have the deepest and narrowest channel possible. As shown above, channel shapes can be very varied depending on the parameters entered. A careful and broad study is essential to understand the impact of each of them. Since the depth of 30µm is mandatory to observe the Cassie-Baxter state, it will be necessary to perform several repetitions per channel to obtain the desired result.

The study of the channels with several repetitions will include the implementation of a movement on the z-axis to try to obtain the greatest possible depth in a minimum of repetitions.

frequency	2 repetitions										3 repetitions						
	Z-axis motion(in µm)										Z-axis motion(in µm)						
	0	5	10	15	20	0	20	20 then 10	Beam energy	0	20	20 then 10	Beam energy	0	20	20 then 10	
5kHz	10µJ	20µJ	10µJ	20µJ	10µJ	20µJ	10µJ	20µJ	10µJ	20µJ	10µJ	20µJ	10µJ	20µJ	10µJ	20µJ	
5kHz	width:17.7 depth:7.63	width:16.7 depth:8.94	width:17.1 depth:8.73	width:19.2 depth:22.9	width:21.9 depth:22.1	width:21 depth:26	width:16.5 depth:10.3	width:21 depth:27.5-30	width:21.8 depth:24.3								
10kHz	width:19.7 depth:22.7	width:18.7 depth:23.6	width:19.2 depth:22.9	width:21.9 depth:22.1	width:21 depth:26	width:21 depth:26	width:16.5 depth:10.3	width:21 depth:27.5-30	width:21.8 depth:24.3								
100kHz	width:19.7 depth:22.7	width:18.7 depth:23.6	width:19.2 depth:22.9	width:21.9 depth:22.1	width:21 depth:26	width:21 depth:26	width:16.5 depth:10.3	width:21 depth:27.5-30	width:21.8 depth:24.3								

Tableau 3 multiple repeats channel data spreadsheet

This study allows us to identify two recipes that will be tested on large surfaces (10mmx10mm). This will allow us to carry out Goniometry tests.

Creation of superhydrophobic surfaces:

Engraved surface with two repetitions:

This engraving is the first engraving of a large surface of this internship. It will allow to adjust the direction of the next tests.

The laser parameters are:

- Energy per pulse: 20 μ J
- Triggering frequency: 10kHz
- Marking speed: 10mm/s
- Number of repetitions: 2
- Movement on the Z axis between repetitions: 20 μ m

The engraving time was approximately 4 hours for a 14mmx10mm surface.

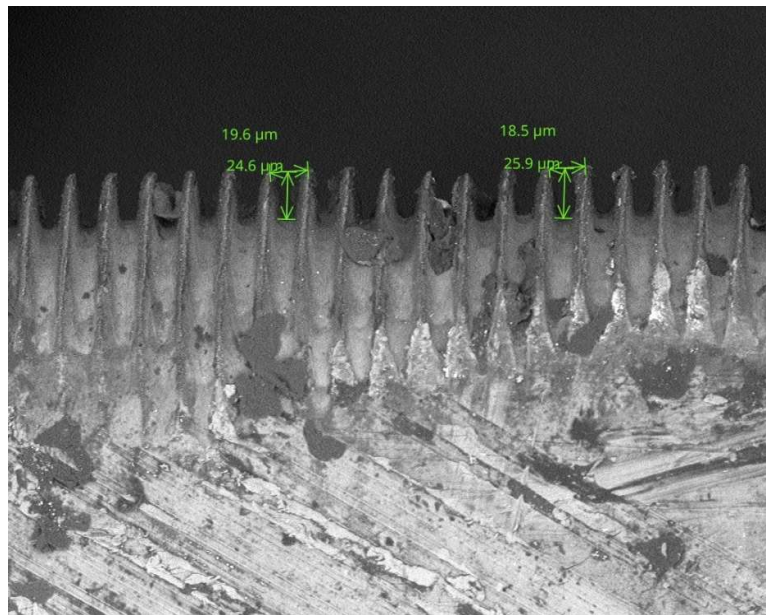


Figure 13 Cross Section two repeats sample

Engraved surface with three repetitions :

This engraving is performed on two different types of surfaces: a polished aluminum sample and a raw aluminum sample. This will allow us to see the impact of polishing on the contact angle.

The laser parameters are:

- Energy per pulse: 20 μ J
- Triggering frequency: 10kHz
- Marking speed: 10mm/s
- Number of repetitions: 3
- Movement on the Z axis between repetitions: 20 μ m

The engraving time was approximately 6 hours per sample

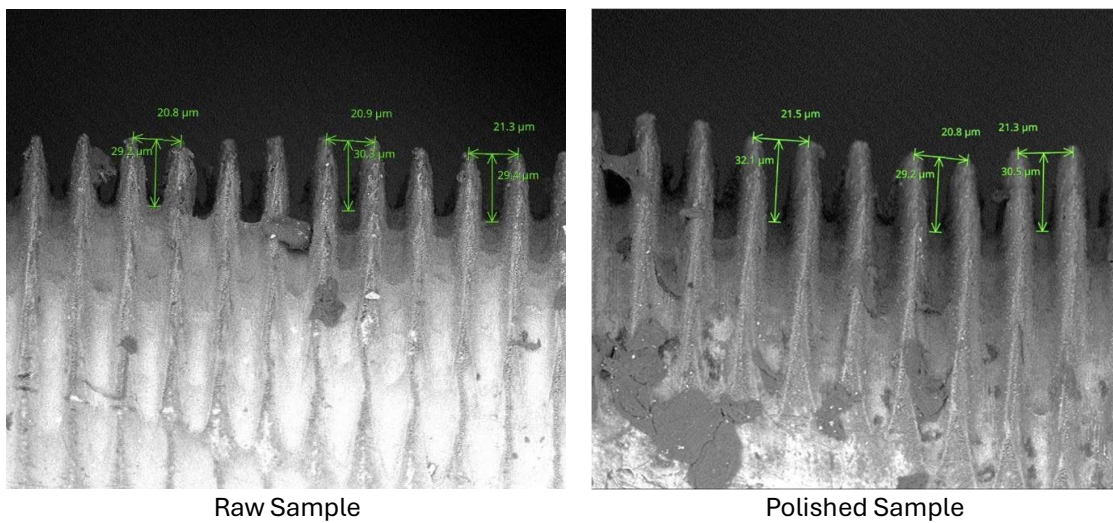


Figure 14 Cross Section three repeats Samples

Measurements and Limits :

Static contact angle test :

Surface two repetitions :

After 48 hours in the rich atmosphere of the airtight box, it is already possible to carry out the goniometry test.

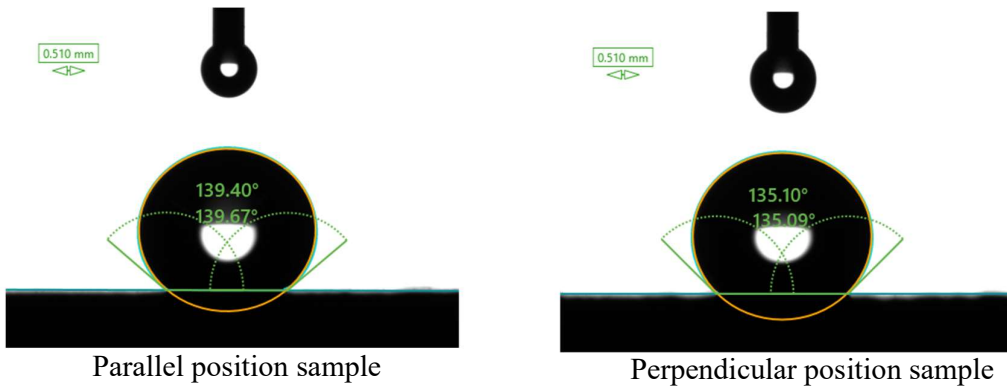


Figure 15 Goniometry test on two repeats sample

The test carried out is encouraging but is not sufficient to move on to the next stage of the project. This is why a second test was carried out with the samples with 3 repetitions per channel.

Surface three repetitions :

The objective of this measurement is to obtain a contact angle close to 150°

And to see the difference between the polished sample and the raw sample.



Figure 16 Goniometry test on three repeats samples

General		Contact Angles			System		Miscellaneous
		Elliptical Fit					
No.	Drop age [s]	CA(EØ) [°]	CA(EL) [°]	CA(ER) [°]	Drop Phase	Substrate	Comment
22	n/a	148,37	148,35	148,38	Water	n/a	para_polished
23	n/a	145,21	145,20	145,22	Water	n/a	para-polished
24	n/a	146,85	146,84	146,86	Water	n/a	perp-polished
25	n/a	144,04	144,04	144,03	Water	n/a	perp-polished
26	n/a	148,64	148,53	148,74	Water	n/a	para-raw
27	n/a	148,91	148,81	149,01	Water	n/a	para-raw
28	n/a	147,06	147,06	147,07	Water	n/a	perp-raw
29	n/a	152,21	152,26	152,16	Water	n/a	perp-raw

Tableau 4 Spreadsheet Contact Angle on three repeats samples

The contact angles are very high regardless of the sample. It is possible to consider these samples superhydrophobic.

Dynamic Contact Angle Measurement :

A complementary test is performed: The dynamic contact angle test consists of making a drop placed on the sample grow and then shrink. The important measurement is the hysteresis which is the difference between the contact angle when the drop grows and the contact angle when the drop decreases in size. The objective is to have a hysteresis of approximately 10°

Results:

Type	Advancing Contact Angle	Receding Contact Angle	Hysteresis
Raw Sample Parallel	159.14°(±5.37°)	153.73°(±4.23°)	9.04°(±4.61°)
Raw Sample Perpendicular	159.81°(±5.87°)	151.75°(±3.69°)	10.39°(±3.98°)
Polished Sample Parallel	148.05°	129.46°	18.59°
Polished Sample Perpendicular	151.58°	144.35°	7.23°

Tableau 5 Spreadsheet Dynamic Contact Angle

The observed contact angles are high and the hysteresis is reasonable. The tests are therefore conclusive.

Limits :

The various tests carried out with these samples make it possible to establish that it is possible to make superhydrophobic surfaces from an aluminum sample without using a chemical coating.

However, the method used is too tedious. Indeed, a 6h engraving for 1.5cm² is not projectable to a plate of 15.5 cm on each side or 240.25 cm². It is therefore necessary to find a way to speed up the process without losing quality.

Study of engravings with a long-range lens :

Study of engravings on single channels :

Classical approach :

The study previously conducted with the short-range lens allows for fewer tests to be performed. It also allows us to know what type of channel is desirable (20µm wide by 30µm deep).

All the tests are recorded here:

frequency	1 repetition									
	Beam energy									
	1µJ	2µJ	5µJ	10µJ	20µJ	30µJ	40µJ	50µJ	60µJ	70µJ
5KHz			width:25 depth:0	width:29.7 depth:0	width:27.8 depth:0		width:32.5 depth:9.82			
10KHz			width:27.5 depth:0	width:29.4 depth:4.55	width:34.5 depth:11.2		width:35.9 depth:13.8		width:31.8 depth:14.3	
20KHz			width:25.8 depth:5.53	width:31.6 depth:8.24	width:35.2 depth:17.5		width:36.3 depth:26.3 SCA: 143-148 ?		width:26.8 depth:27.2	
40KHz				width:24.7 depth:15.8	width:24 depth:26.5		width:26.5 depth: ?		width:30.7 depth: ?	

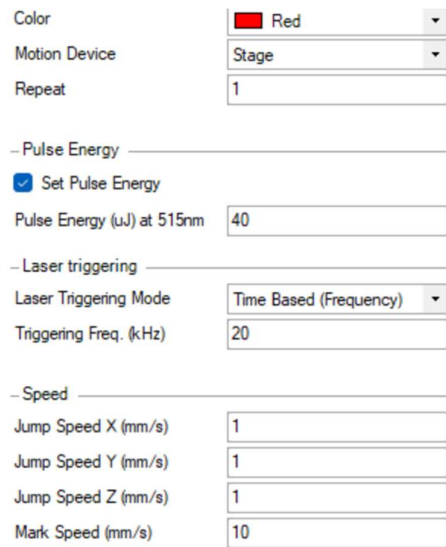
Tableau 6 Spreadsheet datas Long-Range Lens

This table shows that using the short-range lens does not require multiple passes per channel to obtain the desired dimensions. This would already allow the time to be divided by three.

Accelerating the process :

The right lens and the right parameters are now determined. The objective then becomes to optimize all the points that waste time during engraving.

A first observation of the parameters allowed us to determine that there were different types of speeds when adjusting the laser: the marking speed and the jumping speed. The first is the speed of the laser when it is engraving and the second is the speed when it is not engraving.



When the laser finishes engraving a channel, it returns to the starting point of the channel before moving on to the next one.

A similar distance is therefore achieved with both types of speed during engraving.

By default, the speeds are 1mm/s so if we forget to modify the jump speed, we can greatly increase the engraving time.

Figure 17 Laser Marking Parameters Window

Together, these two improvements (lens + jump speed) make it possible to transform a 6h30 engraving into a 25min engraving.

In order to complete this process, a study of the reaction of the channel shape to the increase in speed is carried out. To carry out this test, the recipe of the red cell was taken as a reference and then the frequency and speed are increased with the same factor. (20kHz /10mms then 40kHz/20mms).

1 repetition										
	Beam energy									
speed	1μJ	2μJ	5μJ	10μJ	20μJ	30μJ	40μJ	50μJ	60μJ	
10mm/s							width:29.7 depth:23.2		width:31.5 depth:30.4	
20mm/s							width:30.9 depth:21.9		width:34 depth:26.5	
40mm/s							width:31.5 depth:22		width:32.9 depth:27.7	
60mm/s							width:28.3 depth:36.3		width:30.7 depth:?	
80mm/s							width:27.1 depth:?		width:29.3 depth:?	

Tableau 7 Spreadsheet Speed Test Long-Range Lens

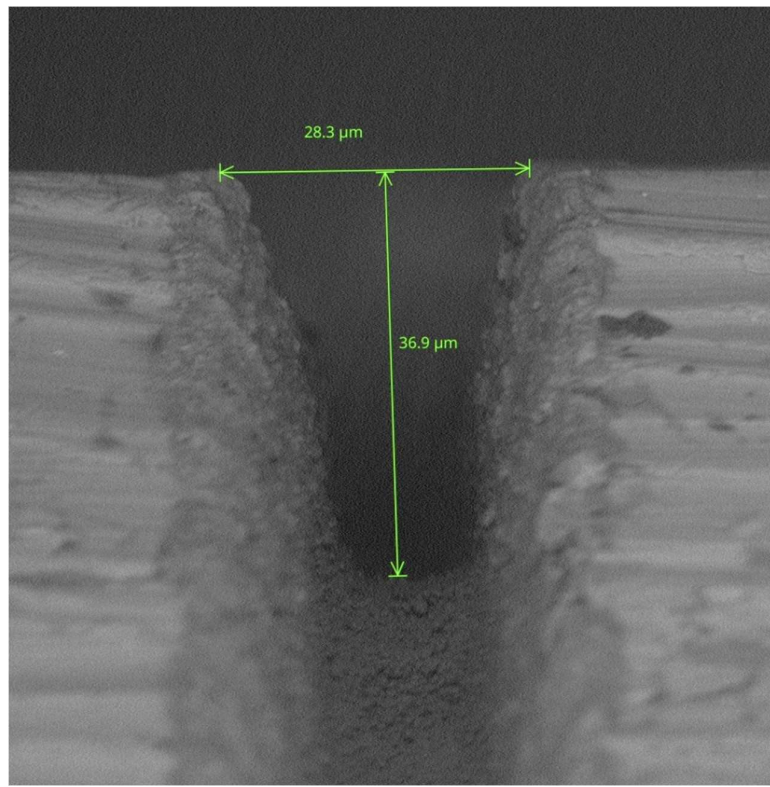


Figure 18 SEM Image of the Single channel of the red cell

This test therefore shows that it is possible to engrave channels at 60mm/s of more than 30μm with a single repetition.

New problems have been detected when the speed increases. Indeed, for high speeds (40mms and +) it is necessary to lengthen the channel after the sample because the laser deceleration zone becomes non-negligible.

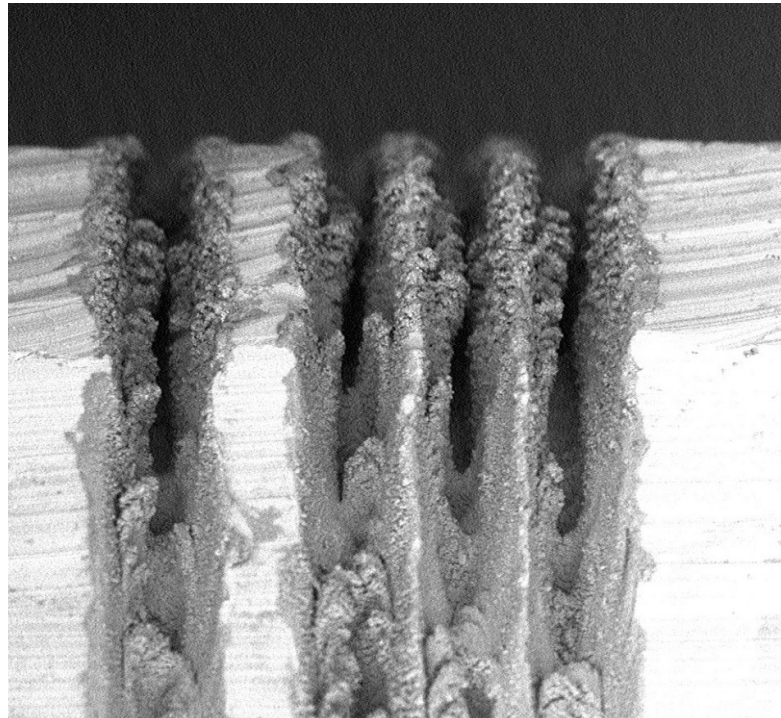


Figure 19 SEM image of the impact of the deceleration of the laser

Here we can see that the end of the channel is damaged because the ratio between speed and firing frequency is impacted by the braking of the laser.

For the moment it is not possible to test higher speeds because the 3-axis displacement platform is limited to 100mm/s.

Creation of superhydrophobic surfaces:

Surface creation with the long-range lens is much faster than with the long-range lens. Indeed, by maintaining a speed of 10mm/s, it is already possible to engrave a surface in 20min.

The laser parameters are:

Energy per pulse: 40μJ

Triggering frequency: 20kHz

Marking speed: 10mm/s

Number of repetitions: 1

The engraving time was approximately 20min for a 10mmx10mm surface.

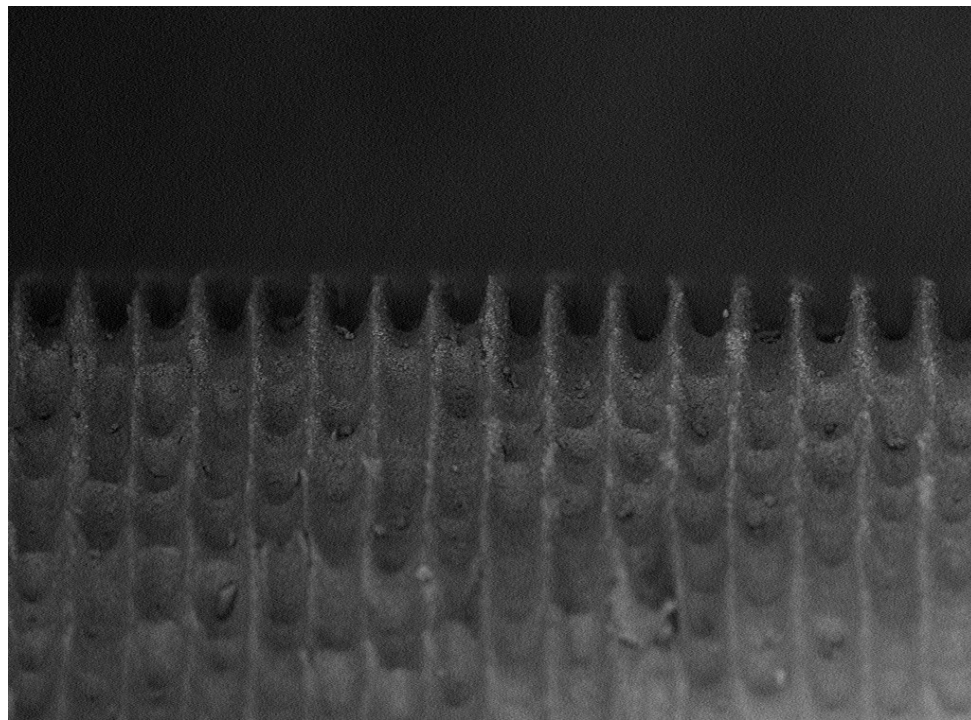


Figure 20 Cross Section of a sample engraved in 25min

Measurements and Limits :

Static measurement of the contact angle :

The goniometry test was performed 48 hours after etching. The sample was stored in the airtight box with the enriched atmosphere.



Figure 21 Goniometry test on 25min engraving Sample

Here is the set of data taken for this sample:

General		Contact Angles			System		Miscellaneous
		Elliptical Fit					
No.	Drop age [s]	CA(EØ) [°]	CA(EL) [°]	CA(ER) [°]	Drop Phase	Substrate	Comment
1	n/a	148,46	148,46	148,47	Water	n/a	para
2	n/a	147,14	147,10	147,17	Water	n/a	para2
3	n/a	148,07	148,01	148,14	Water	n/a	perp
4	n/a	148,52	148,54	148,50	Water	n/a	perp2

Tableau 8 Spreadsheet goniometry test of the 25min engraving sample

Dynamic contact angle measurement

Dynamic contact angle measurement will allow to determine with better accuracy whether the surface is hydrophobic.

Parallel Sample

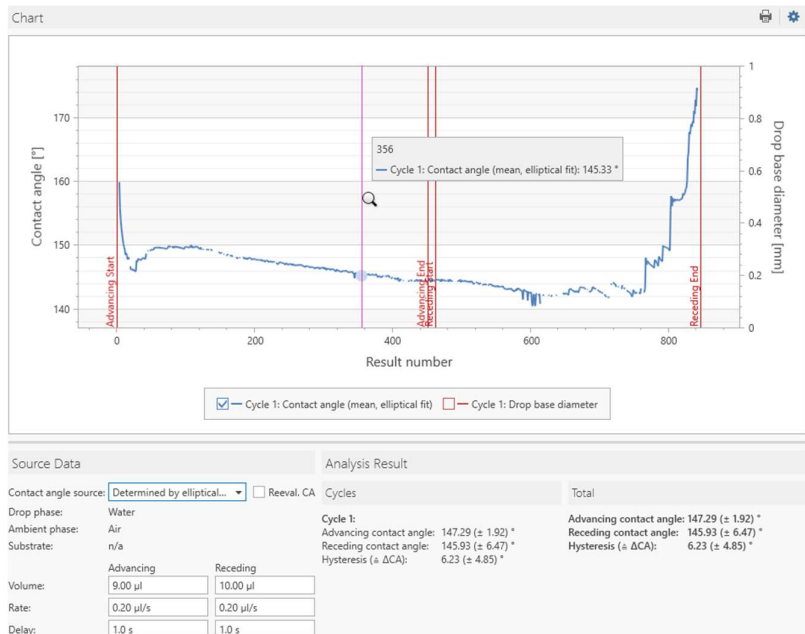


Figure 22 Graph Dynamic Contact angle in parallel position

Perpendicular Sample

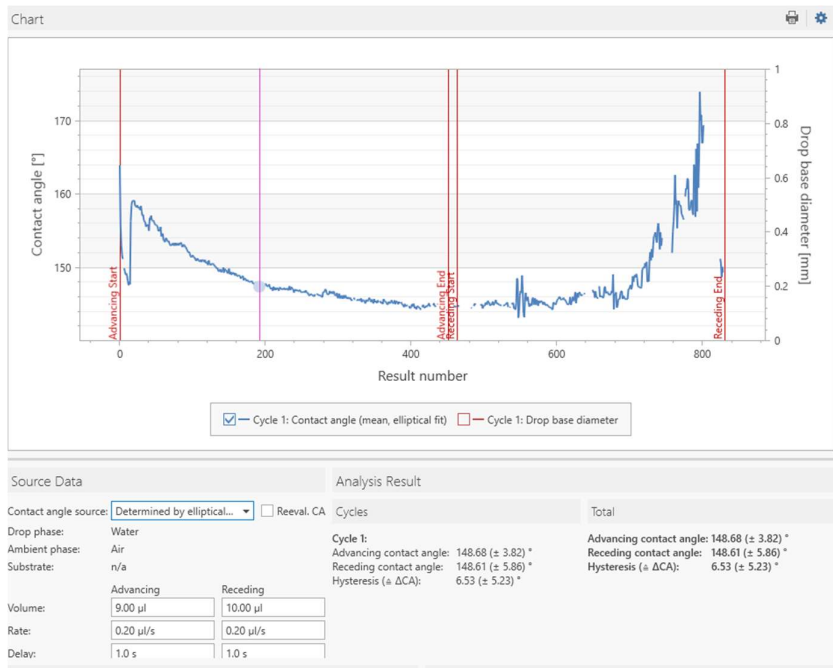


Figure 23 Graph Dynamic Contact Angle perpendicular position

Limits:

This long-range lens study is a real step forward in the desire to engrave large plates for heat exchangers (155mmx155mm). The engraving speed of 60mm could allow this type of plate to be engraved in about 12 hours compared to 6 hours for a 10mmx10mm sample at the beginning of the internship.

However, the project has just reached a new limit. Indeed, the platform for moving the sample under the laser cannot exceed 100mm/s. It is therefore not physically possible to exceed this limit at the moment.

Gradient Creation :*Theory :*

For the moment, surfaces with uniform hydrophobicities have been etched over the entire surface. If the surface is perfectly flat and the drop is deposited gently on the sample, then the contact angle will be high ($>150^\circ$) but the drop will remain on the sample. It is therefore necessary to find a way to give movement to the drop.

To do this, it is possible to vary the space between the channels. Indeed, by gradually increasing the space between the channels, it is possible to create a surface with a hydrophobicity that decreases along its width. The drop will then be attracted to the most hydrophilic area, which will generate movement.

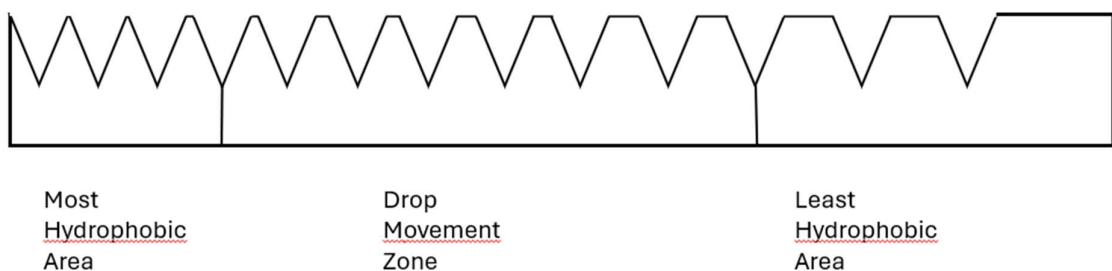


Figure 24 surface gradient example

Study and Measurements :

During this study, four types of gradients were studied: SDG1; SDG1_Mod; LDG4; LDG4_Mod. The LDG4 and SDG1 gradients are modeled by the Cassie-Baxter equation. The fractional surface f is linearly modified to decrease the hydrophobicity progressively. The Mod versions are "home made" gradients. The variation of f follows models determined within the research group. The variation is non-linear.

For each gradient, a video is taken using the goniometer and then it is processed on the Matlab software to obtain different data such as the distance traveled by the drop or the contact angles throughout the movement. Finally, processing this data on Excel makes it possible to obtain different graphs characterizing the gradients.

Gradient SDG1 :

Video Tracking :

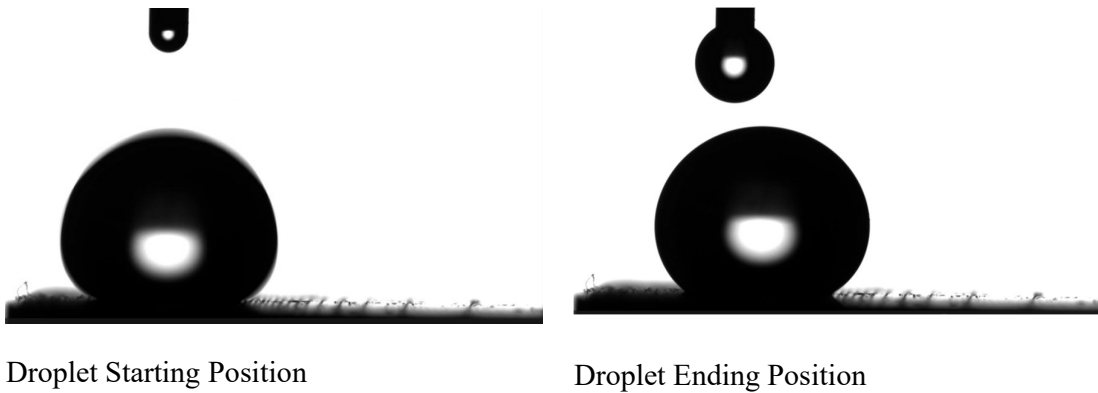
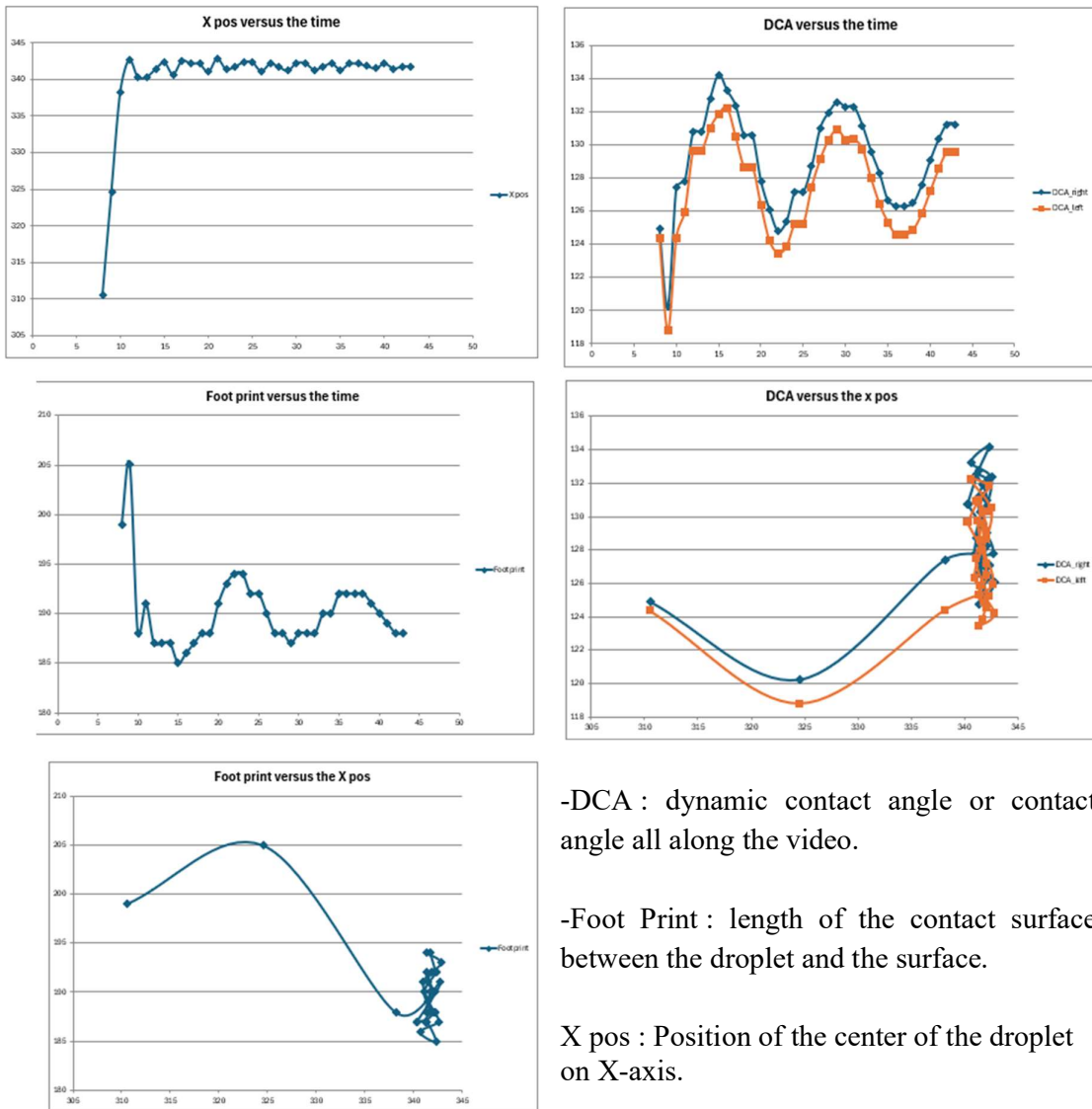


Figure 25 Screenshot Tracking video SDG1

Excel Graphs :

To create Excel graphs, the videos taken must not contain any bounces to avoid having bad contact angles. In Excel, only the angles showing 180° or 0° are removed. This represents the parts where the drop is not in contact with the surface.



-DCA : dynamic contact angle or contact angle all along the video.

-Foot Print : length of the contact surface between the droplet and the surface.

X pos : Position of the center of the droplet on X-axis.

Figure 26 Graphs of the video for gradient SDG1

Interpretation :

The gradient type SDG1 is a gradient starting with a contact angle of 134° and ending its course with a contact angle of about 132° . This gap does not allow for a long displacement.

Gradient SDG1_Mod :

This gradient model is a modified version of SDG1. There are larger gaps between the channels at the end of the gradient.

Video Tracking :

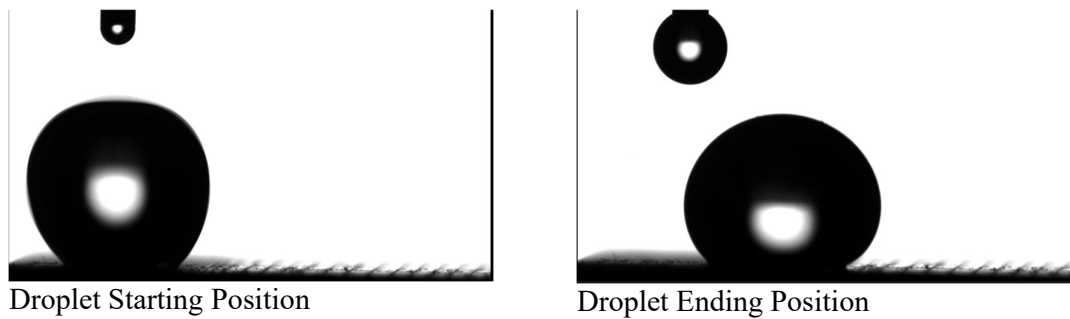
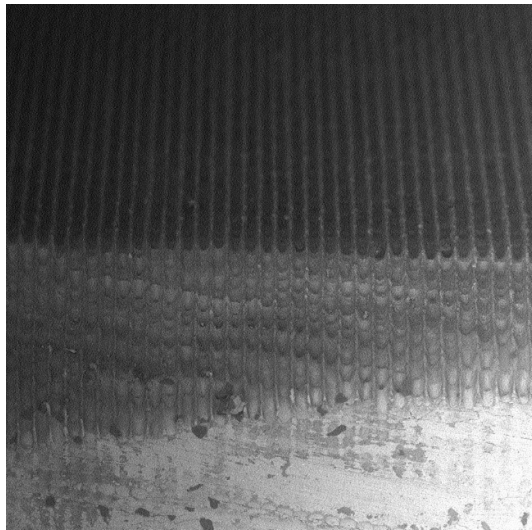


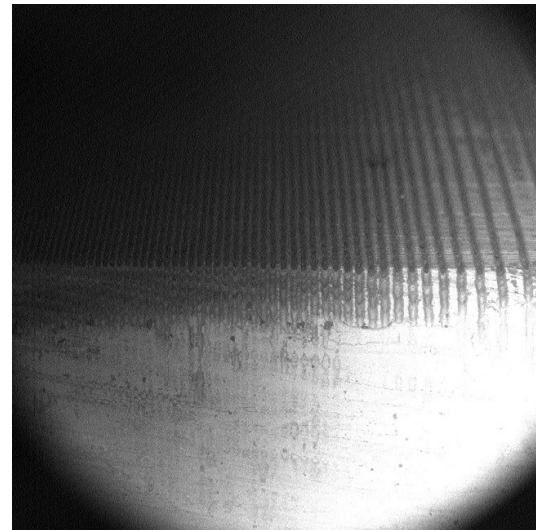
Figure 27 Screenshot of the tracking video of SDG1_Mod gradient

SEM Images :

A study of the gradients under the microscope was carried out on the “Mod” type gradients in order to verify that the test results were consistent with the desired channel type.



Fixed Pitch zone



Gradient Zone

Figure 28 SEM images of SDG1_Mod gradient

Excels Graphs :

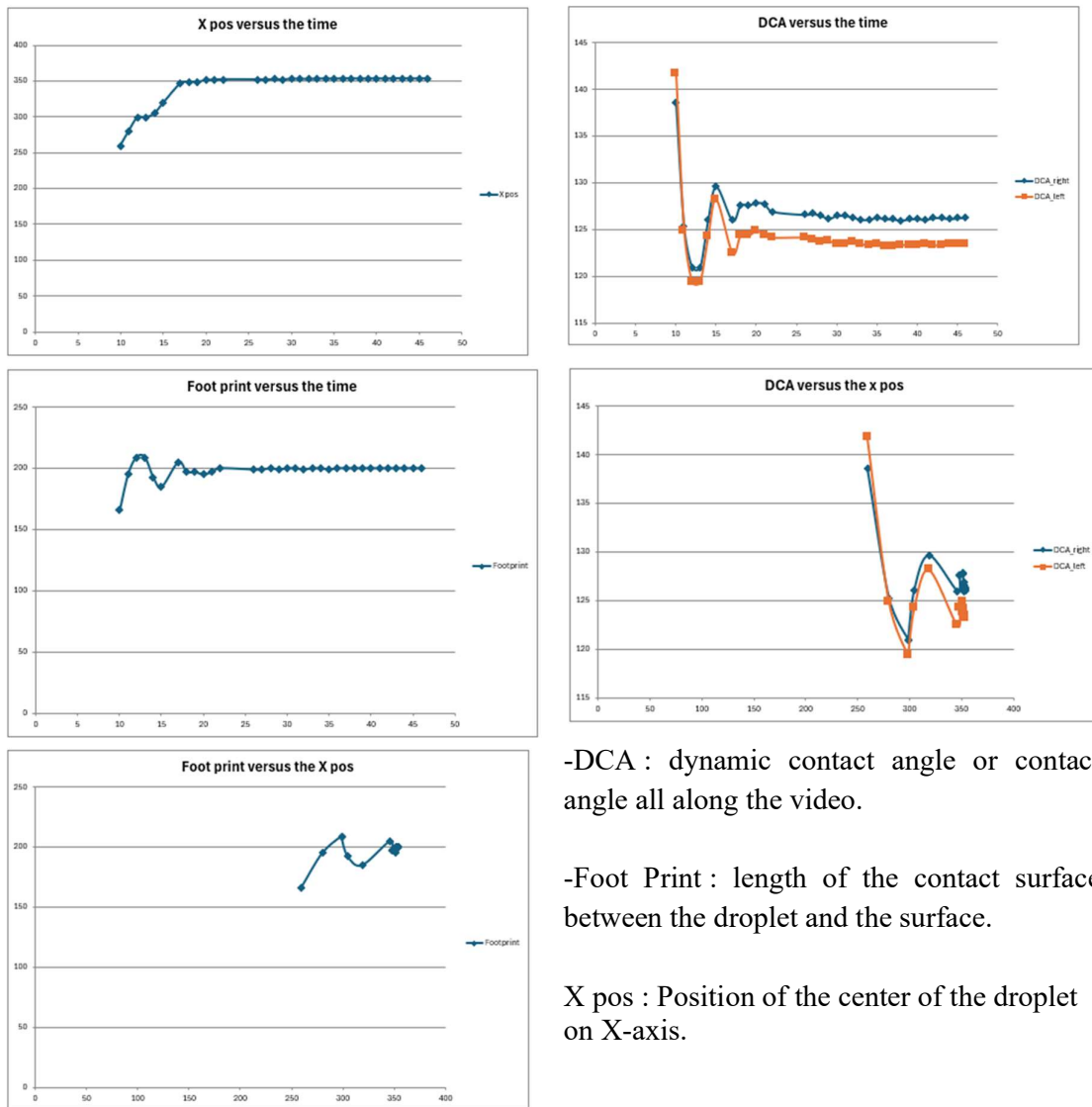


Figure 29 Graphs of the gradient SDG1_Mod

Interpretation :

The gradient SDG1_Mod has a higher starting contact angle than SDG1 and a lower final contact angle. The total displacement is larger.

LDG4 Gradient :

LDG4 is a gradient with more channels. This should help to better distribute the variation in hydrophobicity and extend the distance traveled by the drop.

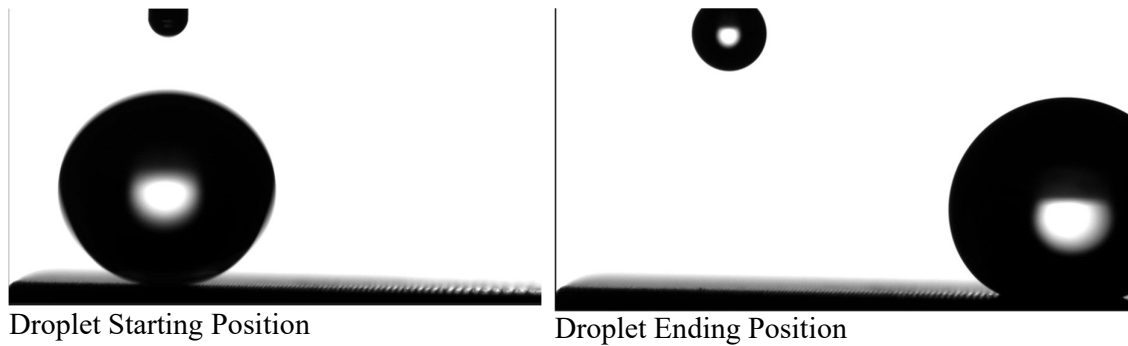
Video Tracking :

Figure 30 Screenshot tracking video of LDG4 gradient

The video shows greater movement along the X axis.

Excel Graphs :

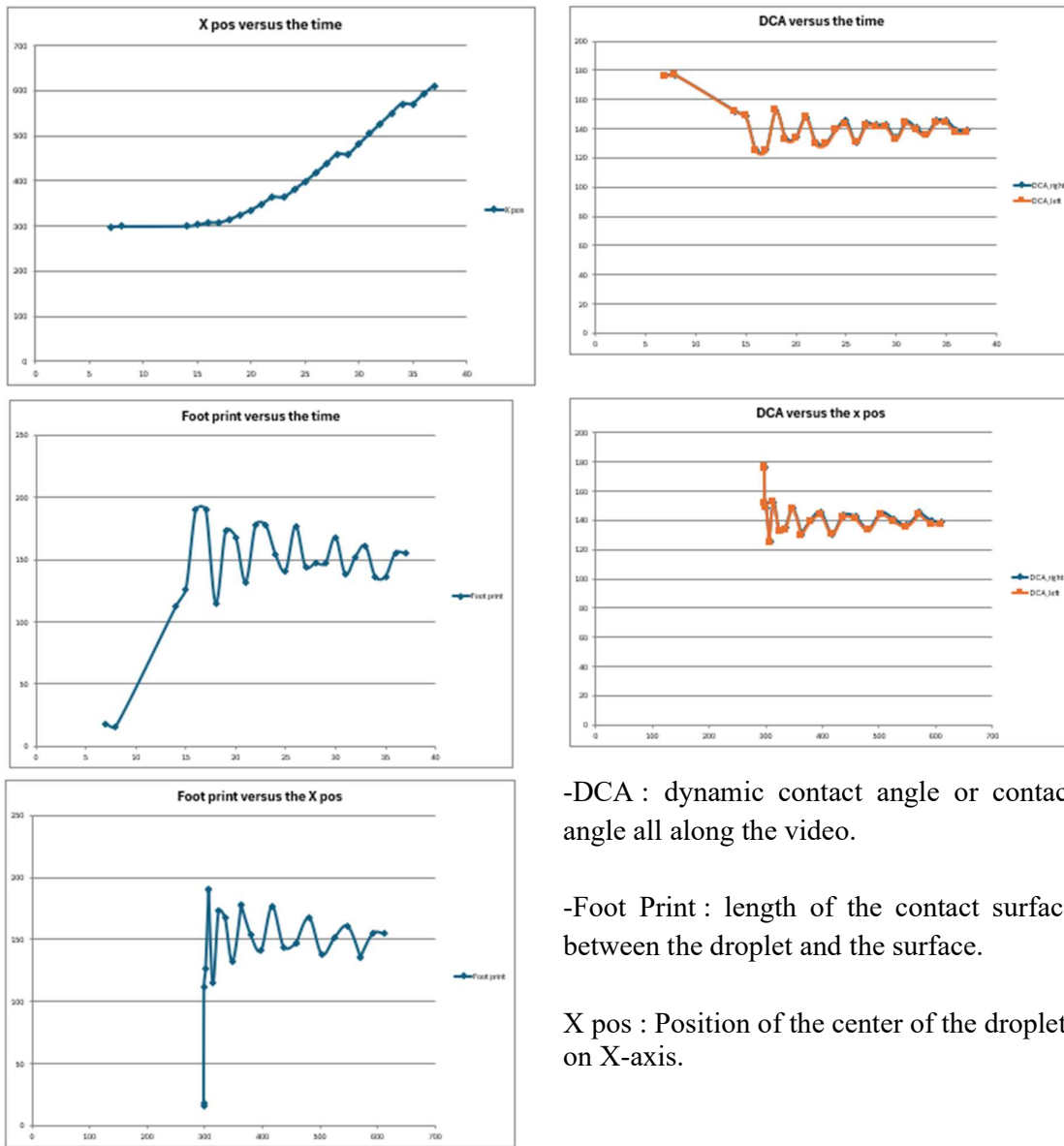


Figure 31 Graphs of the gradient LDG4

The contact angles of LDG4 are higher than those of SDG1. The displacement along the X axis is also much larger. It seems to perform better than SDG1.

Gradient LDG4_Mod :

LDG4_Mod is a modified version of LDG4. The gaps between the channels at the end of the gradient are larger in LDG4_Mod than in LDG4.

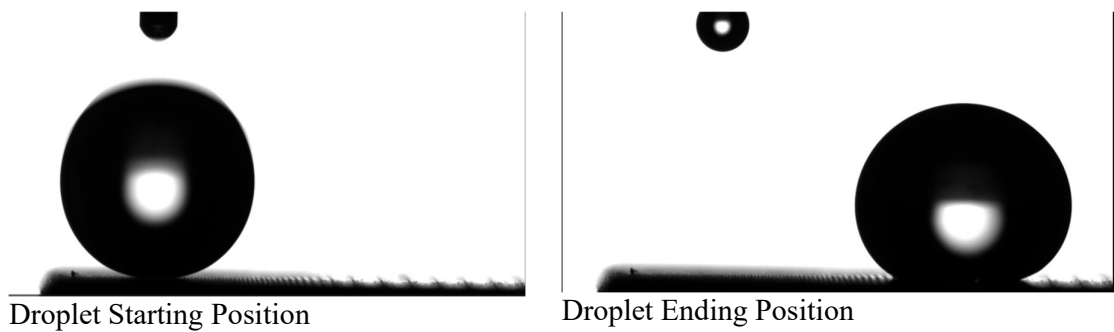
Video Tracking :

Figure 32 Screenshot Tracking video of LDG4_Mod

SEM images :

As for the SDG1_Mod gradient, the LDG4_Mod gradient was studied using a scanning electron microscope.

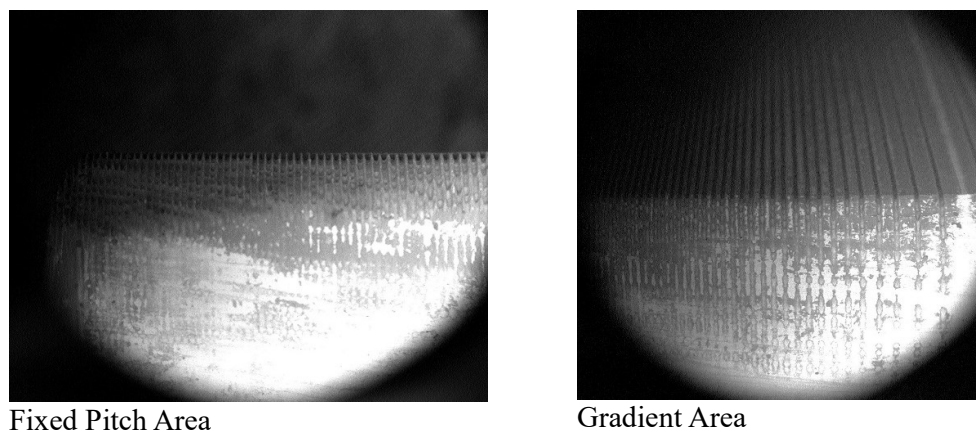


Figure 33 SEM Images of LDG4_Mod

Excel Graphs :

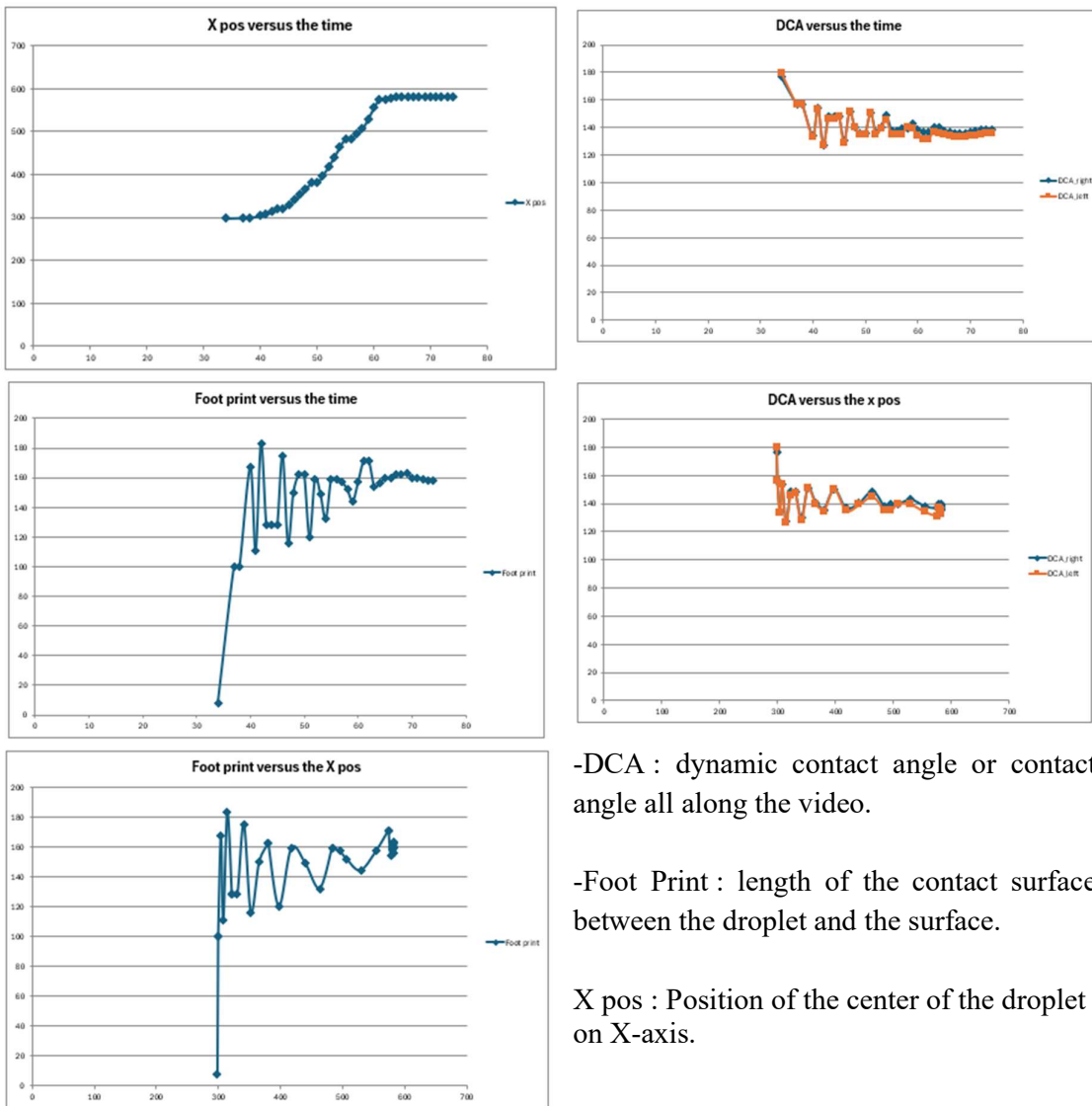


Figure 34 Graphs of the gradient LDG4_Mod

The contact angles of LDG4_Mod remain very high ($>140^\circ$) despite a larger spacing between the channels. This is very encouraging in the perspective of achieving larger surfaces.

Comparison of gradients:

LDG4 and LDG4_Mod gradients have higher contact angles at the beginning and end of the gradient than SDG1 and SDG1_Mod gradients. The distance traveled is also higher for these gradients. They seem to be more promising because the angles close to 140° at the end allow us to hope to lengthen these surfaces to take advantage of a larger range.

Study of Glass Engravings :

The study of glass engravings is part of a desire to broaden the team's knowledge in the engraving of materials as well as their different properties after exposure to the femtosecond laser.

Applications of a hydrophobic glass could be found in the creation of more efficient solar panels.

Study of unique channels :

The engraving of the grooves began with the search for the right ratio between the different laser parameters to obtain channels similar to those engraved on aluminum surfaces.

1 repetition(speed:0.02mm/s)							
Beam energy							
frequency	1μJ	2μJ	5μJ	10μJ	20μJ	30μJ	40μJ
5KHz			width:0 depth:0	width:23.2 depth:16.1	width:29.8 depth:19.9		width:33.2 depth:27.1
10KHz			width:17.1 depth:8.3	width:23.1 depth:11.4 ?	width:31.3 depth:20.5		width:31.3 depth:21.3
20KHz			width:18.5 depth:9.24	width:25.1 depth:8.55 ?	width:34.9 depth: melting		melting
40KHz			width:16.6 depth:7.79	melting	melting		melting

Tableau 9 Spreadsheet Single channels engraving on glass samples

These engravings carried out at 20 $\mu\text{m}/\text{s}$ were intended to show that it was possible to engrave glass. The melting problem is a problem that will be constant throughout the project above a certain energy and frequency.

The speed of 20 μm (Quan Sun, 2008) being far too low to hope to engrave a surface of 10mmx10mm and thus be able to carry out the first goniometry measurements, a speed test must be carried out. For this, the best result of the first experiment is chosen as a reference. The speed will be increased by trying to keep the same ratio between speed and frequency and thus reduce the degradation of the channels.

Speed Test :

	1 repetition (beam energy: 40 μJ)						
	marking speed						
frequency	0.02mm/s	0.05mm/s	0.1mm/s	0.5mm/s	1mm/s	5mm/s	10mm/s
5KHz	width:27.3 depth:21.4	width:27.2 depth:18.3	width:28 depth:21.2	width:27.5 depth:24.2	width:28.5 depth:34.6	width:27.4 depth:14.9	width:30.4 depth:8.76
					width:29.1 depth:22.9	width:27.1 depth:9.21	width:28.7 depth:9.64
10KHz		width:32.1 depth:20.8	width:33.2 depth:18.9	width:31.2 depth:20.2	width:41.8 depth:17.8	width:39.6 depth:19.5	melting
20KHz					melting	melting	melting
40KHz					melting	melting	melting
80KHz					melting	melting	melting
100KHz						melting	melting
120kHz							melting

Tableau 10 Spreadsheet of the speed test on glass sample

The green cell is the reference cell used to compare the two datasets. The red cell is the recipe that seems to give the most promising result.

The recipe in the red cell will be tested on a 15mmx15mm sample..

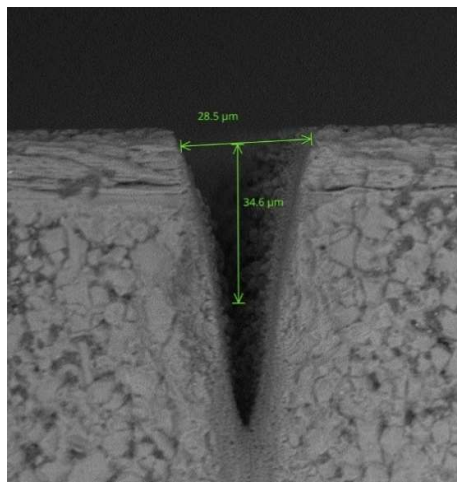


Figure 35 Channel of the red Cell

Creation of an engraved surface :

The laser parameters are:

- Energy per pulse: 40µJ
- Firing frequency: 5kHz
- Engraving speed: 1mm/s
- Number of repetitions: 1

The engraving time was approximately 2 hours for a 15mmx15mm surface.

This engraving was carried out on a sample too large for the microscope. A few channels were engraved on a smaller sample to be able to observe the quality of the engraving.

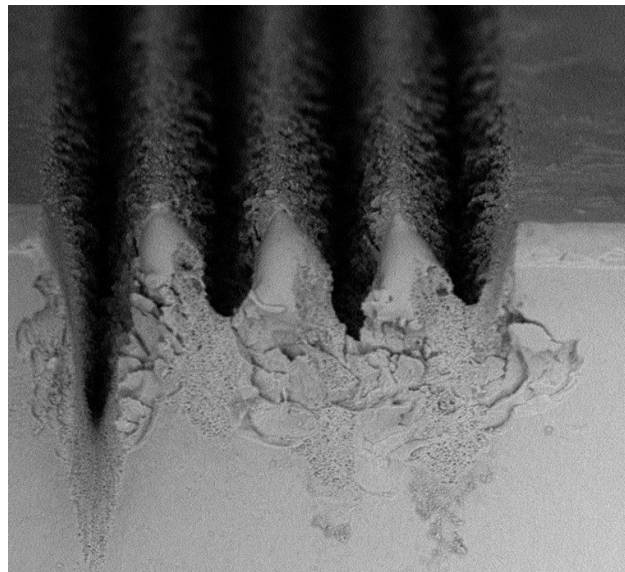


Figure 36 Cross section of an engraved glass sample

Measurements and Limits :

In order to determine the impact of etching on the hydrophobicity of glass samples, a goniometric measurement is performed on a glass sample without etching.

Contact Angle Measurement on Flat Glass :

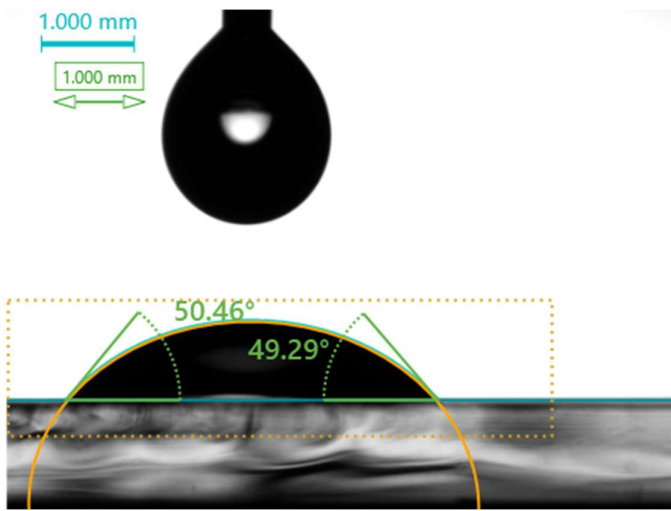


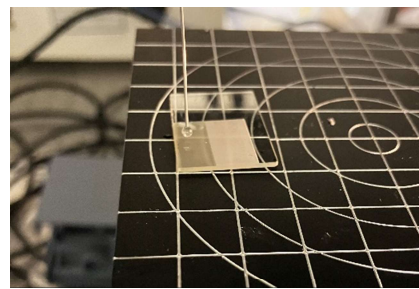
Figure 37 Goniometry test on non-processed glass

Different tests were performed. The values obtained are between 40° and 50° . This result is consistent with what can be found in the literature.

Contact Angle Measurement on Processed Glass :



Sample in perpendicular position



Sample in perpendicular position

Figure 38 Goniometry test on processed glass

The droplet is distributed all along the channels. It is not possible to take a contact angle measurement because the surface is super hydrophilic.

When referring to the Wenzel equation, this is explained because $r=2.6$. However, when the contact angle on a flat surface is approximately equal to 50° we obtain:

$$\cos \theta_W = 2.6 * \cos(50)$$

$$\cos \theta_W = 2.4$$

Above $r=1.55$, the contact angle will always be less than 5° .

Limits :

Despite a model similar to that used to make aluminum samples superhydrophobic, the glass sample had a very different behavior. Although very interesting, super hydrophilicity was not the desired behavior.

Conclusion :

Technical Conclusion :

The objective of this internship was to engrave gradients on aluminum samples. This required studying the impact of laser parameters on the broadest possible spectrum. A "step-by-step" approach was followed in order to keep the best possible understanding of the results.

During this internship, a mapping of the channels was first carried out according to the laser and lens parameters. This mapping now allows for strong control of the laser and the choice of the desired shape.

It was then shown that it was possible to drastically increase the engraving speed for certain patterns by adjusting the triggering frequency and the length of the channel.

Finally, the possibility of engraving "home made" gradients was shown, generating a displacement of the droplet thanks to the pattern.

The creation of superhydrophobic surfaces is now possible in less time and with great ease. The manufacture of gradients requiring control of variable hydrophobicity along the entire surface has also been studied with very encouraging results.

In the broader perspective of creating heat exchanger plates for Doctor Sam Lowrey's research projects, the control of high-speed engraving of aluminum samples (60mm/s +) seems to open very promising doors. Indeed, a 155mmx155mm plate would only take about ten hours compared to several days at the beginning of the internship. It therefore seems to be possible...

Personal Conclusion :

This internship is my first long internship and also my first internship in the engineering and research world. I enjoyed being immersed in an environment that I did not know and in a foreign language. The subject of my internship fascinated me because I see in this subject applications in many areas of the industry, particularly aeronautics (flow of flows, fight against frost on wings). The use of new equipment was a real challenge of adaptability: I had never used the different tools such as the scanning electron microscope or the goniometer. I enjoyed working on process optimization such as engraving acceleration or video data processing for gradients. I'm not sure I'll work in research again, but the engineering world still interests me.

Bibliography

- Jiangyou Long, M. Z. (2014). Superhydrophilicity to superhydrophobicity transition of picosecond.
- Misiuk, K. (2023). Metal topographic surface tension gradients: from idea to implementation.
- Quan Sun, A. S. (2008). Microchannel fabrication in silica glass by femtosecond laser pulses with different central wavelengths.

Appendix :

Appendix 1 :

Poster made for an intern symposium.



Department of Physics

Femtosecond Laser Processing of Aluminium Surfaces for Energy Applications





Current problems



Condensation

Records Pano et al., Nano-structured aluminum surfaces for droplet condensation, 2018



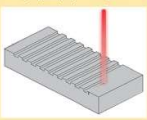
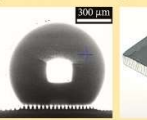
Icing

Dupont, Helping wind turbines cut through ice, 2021

Film-wise condensation decreases the efficiency of heat exchangers, while condensate freezing negatively impacts the performance of both heat exchangers and wind turbines

Possible solution

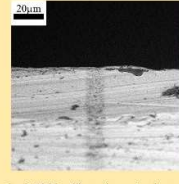
Topography modifications of the initial material (for example, laser etching)

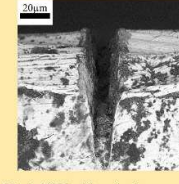

K. Misliuk et al., Langmuir 2022, 38 (4), 1386–1397. DOI: 10.1021/acs.langmuir.1c02517
S. Lowrey et al., Langmuir 2022, 38 (2), 605–619. DOI: 10.1021/acs.langmuir.1c00612

The different parameters of the beam:

- Energy per pulse (μ J)
- Pulse repetition (kHz)
- Marking speed (mm/s)
- Focal distance of the lens (mm)
- The number of repetition per channel

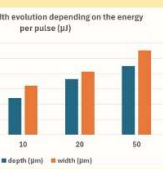


1 μ J, 5kHz, 10mm/s, a single run



20 μ J, 10kHz, 10mm/s, three repetitions

Influence of the laser beam parameters on the topography

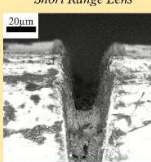


depth and width evolution depending on the energy per pulse (μ J)

Energy per pulse (μ J)	depth (μm)	width (μm)
5	~8	~10
10	~12	~12
20	~18	~18
50	~25	~25

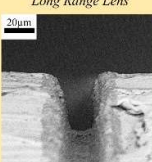
Increasing the energy per pulse allows for manipulating the depth and width of the channels. The energy per pulse can also be decreased by increasing the number of repetitions per channel to increase the channel depth without changing the width.

Short focal distance vs long focal distance lens



Short Range Lens

20 μ J, 10kHz, 10mm/s, two repetitions

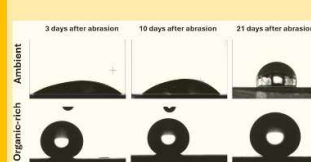


Long Range Lens

20 μ J, 40kHz, 10mm/s, a single run

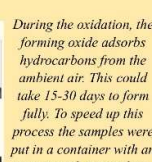
The short-range is a 50mm lens whereas the long-range lens is a 100mm lens. This change allow us to go deeper with one repetition!

Oxidation of metals and its' impact on hydrophobicity



Ambient

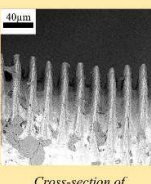
3 days after abrasion 10 days after abrasion 21 days after abrasion



Organic-rich

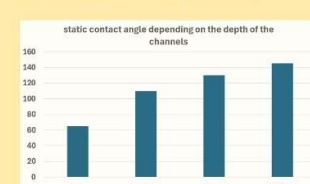
During the oxidation, the forming oxide adsorbs hydrocarbons from the ambient air. This could take 15–30 days to form fully. To speed up this process the samples were put in a container with an organic rich atmosphere.

Large area processing and wetting properties



Cross-section of a 10x10 mm² surface

It may take up to 4 hours to process a 10x10 mm² using the short-range lens and low-energy beam. With the long-range lens and high-energy beam, it takes less than 20 minutes. To have the same shape of the channels it is important to investigate the parameters of the beam thoroughly.



static contact angle depending on the depth of the channels

Depth (μm)	Static Contact Angle (°)
flat	~60
10μm	~110
24μm	~130
30μm	~140



5 μL droplet on a flat and patterned surface

Conclusion

- ✓ Pattern creation is a result of varying laser beam parameters. Understanding the impact of each allows making various topography that leads to different wetting properties.
- ✓ Optimising the laser beam parameters will also help reduce the time needed to process larger areas as the laser ablation technique suitable for making full heat exchangers with outstanding wetting properties without using any coatings.
- ✓ This technique could be extended to other materials such as glass for applications in the energy field (solar panels).

Further reading

- o K. Misliuk et al., Langmuir 2022, 38 (4), 1386–1397. DOI: 10.1021/acs.langmuir.1c02517
- o S. Lowrey et al., Langmuir 2022, 38 (2), 605–619. DOI: 10.1021/acs.langmuir.1c00612
- o J. Long et al., J. Colloid Interface Sci., J. Colloid Interface Sci. 2015, 441, 1–9. DOI: 10.1016/j.jcis.2014.11.015
- o K. Misliuk et al., Langmuir 2022, 38 (6), 1954–1965. DOI: 10.1021/acs.langmuir.1c02518
- o K. Misliuk et al., Phys. Fluids 2023, 35 (2), 024108. DOI: 10.1063/5.0137910.

Acknowledgements

The authors would like to gratefully acknowledge financial support from the Ministry of Business, Innovation and Employment (contract 17548).

Appendix 2 :

All samples processed during the internship are stored in the container and the fruit acid bottle.

